

Modulation of Multimetal Complexation Behavior of Tetraoxime Ligand by Covalent Transformation of Olefinic Functionalities

Shigehisa Akine, Satoko Kagiya, and Tatsuya Nabeshima*

Graduate School of Pure and Applied Sciences, University of Tsukuba, Tsukuba, Ibaraki 305-8571, Japan

Received October 7, 2009

A new multimetal complexation system that can change its complexation behavior by C–C bond formation has been developed. The acyclic tetraoxime ligand H_4L^1 having two terminal allyl groups was synthesized. The olefin metathesis of H_4L^1 selectively produced $trans-H_4L^2$ while the reaction of $[L^1Zn_2Ca]$ exclusively afforded $cis-H_4L^2$. The saturated analogue H_4L^3 was synthesized by hydrogenation. The complexation of the ligands H_4L ($L = L^1, trans-L^2, cis-L^2, L^3$) with zinc(II) acetate (3 equiv) yielded the trinuclear complexes $[LZn_3]$ with a similar trinuclear core bridged by acetato ligands. Whereas the formation process of $[L^1Zn_3]$ having an acyclic ligand was highly cooperative, the macrocyclic analogues $[LZn_3]$ ($L = trans-L^2, cis-L^2, L^3$) were formed in a stepwise fashion via the intermediate 2:3 complex $[(HL)_2Zn_3]$. The trinuclear complexes $[LZn_3]$ ($L = L^1, trans-L^2, cis-L^2, L^3$) can recognize alkaline earth metal ions via site-selective metal exchange. The acyclic $[L^1Zn_3]$ selectively recognizes Ca^{2+} , while the cyclic $[trans-L^2Zn_3]$ showed a Ba^{2+} selectivity. The metal exchange of $[LZn_3]$ ($L = L^1, trans-L^2, cis-L^2, L^3$) with La^{3+} efficiently occurred to give $[LZn_2La]$, but the $trans$ -olefin linker of the $[trans-L^2Zn_2La]$ significantly deforms the structure in such a way that one of the salicylaldoxime moieties does not participate in the coordination. Consequently, the chemical transformation of the olefinic moiety significantly affects the multimetal complexation behavior of the tetraoxime ligands.

Introduction

Macrocyclic ligands play an important role in the selective strong binding with metal ions in coordination chemistry. The difference between the acyclic and cyclic ligands during the coordination behavior mainly arises from the preorganization of the coordinating atoms for the metal ions (macrocyclic effect).¹ In general, the cyclic derivatives show a stronger binding ability than the acyclic ones, and the higher selectivity is achieved using the cyclic framework. Highly selective metal coordination in crown ether chemistry is mainly based on this principle.

Therefore, conversion from an acyclic structure to cyclic ones is expected to significantly change the metal complexation ability. To date, several cyclization methods, such as metal coordination,² disulfide bond formation,³

and photodimerization,⁴ have been used for the conversion to regulate the metal complexation ability. These methods are useful as a tool for the interconversion because covalent and coordination bonds can be formed under mild conditions.

We have designed a system that uses ruthenium-catalyzed olefin metathesis⁵ to convert acyclic ligands to cyclic structures. Nowadays, the synthesis of various supramolecular systems utilizes the olefin metathesis as a tool for cyclization.^{6–8} Olefin metathesis of two terminal olefins produces an internal olefin with a *cis* or *trans* configuration under mild conditions, and the internal olefins are easily converted to the saturated analogue by hydrogenation. Consequently, we can obtain three kinds of cyclic host molecules (*cis* and *trans* olefin, and the saturated analogue) by ring-closing olefin metathesis from a host molecule bearing terminal olefin moieties at both ends. In this strategy, it is important to

*To whom correspondence should be addressed. E-mail: nabesima@chem.tsukuba.ac.jp. Fax: +81-29-853-4507. Phone: +81-29-853-4507.

(1) Cabbiness, D. K.; Margerum, D. W. *J. Am. Chem. Soc.* **1969**, *91*, 6540–6541.

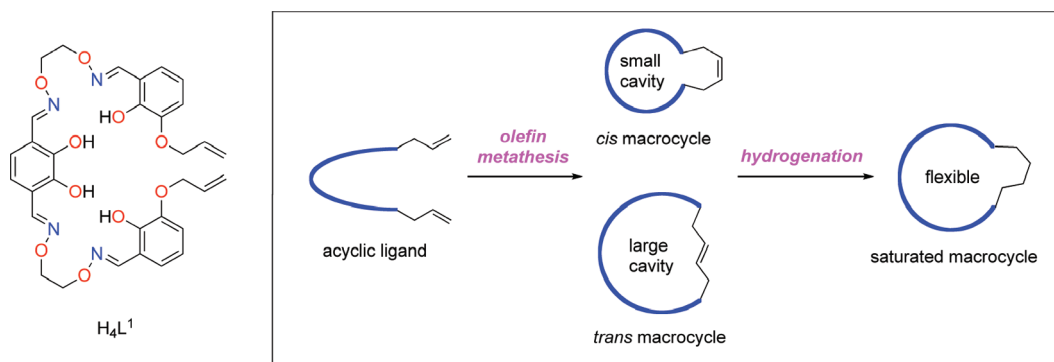
(2) (a) Nabeshima, T.; Inaba, T.; Furukawa, N. *Tetrahedron Lett.* **1987**, *28*, 6211–6214. (b) Nabeshima, T.; Inaba, T.; Furukawa, N.; Hosoya, T.; Yano, Y. *Inorg. Chem.* **1993**, *32*, 1407–1416.

(3) (a) Raban, M.; Greenblatt, J.; Kandil, F. *J. Chem. Soc., Chem. Commun.* **1983**, 1409–1411. (b) Shinkai, S.; Inuzuka, K.; Miyazaki, O.; Manabe, O. *J. Am. Chem. Soc.* **1985**, *107*, 3950–3955.

(4) (a) Desvergne, J.-P.; Bouas-Laurent, H. *J. Chem. Soc., Chem. Commun.* **1978**, 403–404. (b) Xu, M.; Wu, L.-Z.; Zhang, L.-P.; Tung, C.-H. *Tetrahedron Lett.* **2001**, *42*, 9249–9252. (c) Yamashita, I.; Fujii, M.; Kaneda, T.; Misumi, S.; Otsubo, T. *Tetrahedron Lett.* **1980**, *21*, 541–544.

(5) For reviews, see: (a) Trnka, T. M.; Grubbs, R. H. *Acc. Chem. Res.* **2001**, *34*, 18–29. (b) Grubbs, R. H. *Tetrahedron* **2004**, *60*, 7117–7140. (c) Grubbs, R. H. *Angew. Chem., Int. Ed.* **2006**, *45*, 3760–3765.

(6) For interlocked compounds prepared by olefin metathesis, see: (a) Dietrich-Buchecker, C.; Rapenne, G.; Sauvage, J.-P. *Coord. Chem. Rev.* **1999**, *185–186*, 167–176. (b) Aricó, F.; Badjic, J. D.; Cantrill, S. J.; Flood, A. H.; Leung, K. C.-F.; Liu, Y.; Stoddart, J. F. *Top. Curr. Chem.* **2005**, *249*, 203–259. (c) Dietrich-Buchecker, C.; Jimenez-Molero, M. C.; Sartor, V.; Sauvage, J.-P. *Pure Appl. Chem.* **2003**, *75*, 1383–1393. (d) Molokanova, O.; Bogdan, A.; Vysotsky, M. O.; Bolte, M.; Ikai, T.; Okamoto, Y.; Böhmer, V. *Chem.—Eur. J.* **2007**, *13*, 6157–6170.

Scheme 1. Olefin Metathesis and Hydrogenation for the Structural Conversion to Regulate the Multimetal Complexation Behavior

develop a method to selectively obtain the *cis* or *trans* isomer of the olefinic macrocycle. We have preliminarily reported that an oligometallic template strategy is effective for obtaining the two isomers of a tetraoxime ligand for multimetal complexation.⁹ The parent tetraoxime ligand with methoxy groups instead of olefinic moieties is converted to the trinuclear metallohost via cooperative complexation, exhibiting a cation recognition ability through the metal exchange process.¹⁰ In this study, we investigated the complexation ability and selectivity during the transmetalation-based ion recognition of three kinds of macrocyclic molecules, olefins (*trans* and *cis*) and saturated analogues, which are obtained from the acyclic tetraoxime ligand H_4L^1 via the olefin metathesis (Scheme 1).

Experimental Section

General Procedures. All experiments were carried out in air unless otherwise noted. Dichloromethane and tetrahydrofuran (THF) were distilled under argon atmosphere from calcium hydride and sodium benzophenone ketyl, respectively, prior to use. Commercial chloroform, methanol, and ethanol were used without purification. All chemicals were of reagent grade and used as received. Column chromatography was performed with Kanto Chemical silica gel 60N (spherical, neutral). Gel permeation chromatography (GPC) was performed by an LC-908W equipped with JAI gel 1H + 2H columns (Japan Analytical Industry) with chloroform as eluent. Melting points were determined on a Yanaco melting point apparatus and not corrected. 1H and ^{13}C NMR spectra were recorded on a Bruker ARX400

(400 and 100 MHz) spectrometer. Mass spectra (ESI-TOF, positive mode) were recorded on an Applied Biosystems QStar Pulsar *i* spectrometer. Absorption spectra were recorded on a JASCO Ubest V560 spectrometer.

Materials. 2,3-Dihydroxybenzene-1,4-dicarbaldehyde (**3**),^{10e} 3-allyloxy-2-hydroxybenzaldehyde (**1**),¹¹ and 1,2-bis(aminooxy)ethane¹² were prepared according to the literature. Benzylidenebis(tricyclohexylphosphine)dichlororuthenium (Grubbs I) and benzylidene[1,3-bis(2,4,6-trimethylphenyl)-2-imidazolidinylidene]dichloro(tricyclohexylphosphine)ruthenium (Grubbs II) were purchased from Aldrich.

Synthesis of 3-Allyloxy-2-hydroxybenzaldehyde *O*-(2-(aminooxy)ethyl) Oxime (2**).** A solution of 3-allyloxy-2-hydroxybenzaldehyde (**1**, 843 mg, 4.73 mmol) in ethanol (30 mL) was added dropwise to a stirred solution of 1,2-bis(aminooxy)ethane (962 mg, 10.4 mmol) in ethanol (15 mL) at 60 °C, and the resulting solution was stirred for further 1 h at the same temperature. After removal of the solvent, the residue was subjected to column chromatography on silica gel (eluent, hexane/ethyl acetate, 1:1) to yield the oxime **2** (950 mg, 80%) as colorless crystals; mp 70–71 °C, 1H NMR (400 MHz, $CDCl_3$) δ 3.95–3.98 (m, 2H), 4.35–4.38 (m, 2H), 4.64 (dt, J = 5.4, 1.4 Hz, 2H), 5.29 (dq, J = 10.4, 1.4 Hz, 1H), 5.42 (dq, J = 17.2, 1.4 Hz, 1H), 5.51 (brs, 2H), 6.10 (ddt, J = 17.2, 10.4, 5.4 Hz, 1H), 6.80–6.85 (m, 2H), 6.91–6.95 (m, 1H), 8.23 (s, 1H), 9.82 (s, 1H). ^{13}C NMR (100 MHz, $CDCl_3$) δ 70.17 (CH_2), 72.71 (CH_2), 73.70 (CH_2), 115.79 (CH), 116.86 (C), 117.95 (CH_2), 119.33 (CH), 122.76 (CH), 133.29 (CH), 147.04 (C), 147.59 (C), 151.43 (CH). Anal. Calcd for $C_{12}H_{16}N_2O_4$: C, 57.13; H, 6.39; N, 11.10. Found: C, 57.24; H, 6.44; N, 10.95.

Synthesis of Tetraoxime Ligand H_4L^1 . A solution of 2,3-dihydroxybenzene-1,4-dicarbaldehyde (**3**, 368 mg, 2.21 mmol) in ethanol (40 mL) was added slowly to a solution of oxime **2** (1.17 g, 4.64 mmol) in ethanol (35 mL) at 60 °C, and the solution was stirred for 1 h at the same temperature. After the solution was allowed to stand overnight at room temperature, precipitates were collected on a suction filter to afford H_4L^1 (1.17 g, 83%) as colorless crystals; mp 122–125 °C. 1H NMR (400 MHz, $CDCl_3$) δ 4.47–4.52 (m, 8H), 4.63 (dt, J = 5.4, 1.5 Hz, 4H), 5.29 (dq, J = 10.4, 1.5 Hz, 2H), 5.42 (dq, J = 17.2, 1.5 Hz, 2H), 6.09 (ddt, J = 17.2, 10.4, 5.4 Hz, 2H), 6.76 (s, 2H), 6.79–6.86 (m, 4H), 6.92 (dd, J = 7.2, 2.2 Hz, 2H), 8.23 (s, 2H), 8.26 (s, 2H), 9.59 (s, 2H), 9.68 (s, 2H). ^{13}C NMR (100 MHz, $CDCl_3$) δ 70.21 (CH_2), 73.03 (CH_2), 73.20 (CH_2), 116.01 (CH), 116.75 (C), 117.61 (C), 117.90 (CH_2), 119.36 (CH), 120.75 (CH), 122.90 (CH), 133.29 (CH), 145.78 (C), 147.01 (C), 147.62 (C), 151.33 (CH), 151.88 (CH). Anal. Calcd for $C_{32}H_{34}N_4O_{10}$: C, 60.56; H, 5.40; N, 8.83. Found: C, 60.37; H, 5.42; N, 8.73.

(7) For ring-closing metathesis using a template, see: (a) Clark, T. D.; Ghadiri, M. R. *J. Am. Chem. Soc.* **1995**, *117*, 12364–12365. (b) Ng, P. L.; Lambert, J. N. *Synlett* **1999**, 1749–1750. (c) Cardullo, F.; Calama, M. C.; Snellink-Ruël, B. H. M.; Weidmann, J.-L.; Bielejewska, A.; Fokkens, R.; Nibbering, N. M. M.; Timmerman, P.; Reinhoudt, D. N. *Chem. Commun.* **2000**, 367–368. (d) Chuchuryukin, A. V.; Dijkstra, H. P.; Suijkerbuijk, B. M. J. M.; Klein Gebbink, R. J. M.; van Klink, G. P. M.; Mills, A. M.; Spek, A. L.; van Koten, G. *Angew. Chem., Int. Ed.* **2003**, *42*, 228–230. (e) Yang, X.; Gong, B. *Angew. Chem., Int. Ed.* **2005**, *44*, 1352–1356. (f) Kaucher, M. S.; Harrell, W. A., Jr.; Davis, J. T. *J. Am. Chem. Soc.* **2006**, *128*, 38–39. (g) Nawara, A. J.; Shima, T.; Hampel, F.; Gladysz, J. A. *J. Am. Chem. Soc.* **2006**, *128*, 4962–4963. (h) Hiraoka, S.; Yamauchi, Y.; Arakane, R.; Shionoya, M. *J. Am. Chem. Soc.* **2009**, *131*, 11646–11647.

(8) For ring-closing metathesis from a helical structure, see: Blackwell, H. E.; Sadowsky, J. D.; Howard, R. J.; Sampson, J. N.; Chao, J. A.; Steinmetz, W. E.; O'Leary, D. J.; Grubbs, R. H. *J. Org. Chem.* **2001**, *66*, 5291–5302.

(9) Akine, S.; Kagiya, S.; Nabeshima, T. *Inorg. Chem.* **2007**, *46*, 9525–9527.

(10) (a) Akine, S.; Taniguchi, T.; Nabeshima, T. *Angew. Chem., Int. Ed.* **2002**, *41*, 4670–4673. (b) Akine, S.; Taniguchi, T.; Saiki, T.; Nabeshima, T. *J. Am. Chem. Soc.* **2005**, *127*, 540–541. (c) Akine, S.; Matsumoto, T.; Taniguchi, T.; Nabeshima, T. *Inorg. Chem.* **2005**, *44*, 3270–3274. (d) Akine, S.; Taniguchi, T.; Nabeshima, T. *Tetrahedron Lett.* **2006**, *47*, 8419–8422. (e) Akine, S.; Taniguchi, T.; Nabeshima, T. *J. Am. Chem. Soc.* **2006**, *128*, 15765–15774.

(11) Kilényi, S. N.; Mahaux, J.-M.; van Durme, E. *J. Org. Chem.* **1991**, *56*, 2591–2594.

(12) Dixon, D. W.; Weiss, R. H. *J. Org. Chem.* **1984**, *49*, 4487–4494.

Synthesis of *trans*-H₄L². Under nitrogen atmosphere, a solution of Grubbs I (16.9 mg, 0.0205 mmol) in dichloromethane (20 mL) was added to a solution of H₄L¹ (130.5 mg, 0.206 mmol) in dichloromethane (150 mL). The solution was stirred for 46 h at room temperature keeping the flask in the dark. After the removal of the solvent, the residue was recrystallized from chloroform/methanol to give *trans*-H₄L² (84.8 mg, 68%) as colorless crystals, mp 207–209 °C. ¹H NMR (400 MHz, CDCl₃) δ 4.45–4.47 (m, 4H), 4.50–4.52 (m, 4H), 4.61–4.62 (m, 4H), 6.10–6.12 (m, 2H), 6.79 (t, *J* = 7.6 Hz, 2H), 6.80 (s, 2H), 6.83 (dd, *J* = 7.6, 2.1 Hz, 2H), 6.91 (dd, *J* = 7.6, 2.1 Hz, 2H), 8.19 (s, 2H), 8.27 (s, 2H), 9.56 (s, 2H), 9.94 (s, 2H). ¹³C NMR (100 MHz, CDCl₃) δ 69.37 (CH₂), 72.37 (CH₂), 74.99 (CH₂), 116.80 (CH), 116.97 (C), 117.73 (C), 119.19 (CH), 121.24 (CH), 123.24 (CH), 128.31 (CH), 145.69 (C), 146.93 (C), 148.06 (C), 150.95 (CH), 152.90 (CH). ESI-MS *m/z* 629.2 for [M + Na]⁺. Anal. Calcd for C₃₀H₃₀N₄O₁₀: C, 59.40; H, 4.99; N, 9.24. Found: C, 59.23; H, 5.03; N, 9.16.

Synthesis of *cis*-H₄L². Under nitrogen atmosphere, a solution of Grubbs II (25.5 mg, 0.030 mmol) in THF (15 mL) was added to a solution of [L¹Zn₂Ca(OAc)₂] (137.9 mg, 0.15 mmol) in THF (15 mL). The solution was refluxed for 9 h keeping the flask in the dark. After the removal of the solvent, the residue was treated with chloroform (36 mL) and hydrochloric acid (1 M, 36 mL), and the mixture was stirred for 1 h at room temperature. The organic layer was separated, and the aqueous layer was extracted with chloroform. The combined organic layer was dried over anhydrous magnesium sulfate and concentrated to dryness. The residue was recrystallized from chloroform/methanol to give *cis*-H₄L² (58.4 mg, 64%) as colorless crystals, mp 180–182 °C; ¹H NMR (400 MHz, CDCl₃) δ 4.46–4.48 (m, 4H), 4.51–4.52 (m, 4H), 4.73 (d, *J* = 2.8 Hz, 4H), 5.97 (t, *J* = 2.8 Hz, 2H), 6.61 (s, 2H), 6.70 (t, *J* = 7.8 Hz, 2H), 6.76 (dd, *J* = 7.8, 1.4 Hz, 2H), 6.80 (dd, *J* = 7.8, 1.4 Hz, 2H), 8.16 (s, 2H), 8.17 (s, 2H), 9.51 (s, 2H), 9.98 (s, 2H). ¹³C NMR (100 MHz, CDCl₃) δ 66.01 (CH₂), 73.72 (CH₂), 75.99 (CH₂), 115.12 (CH), 116.59 (C), 117.45 (C), 119.10 (CH), 120.89 (CH), 122.83 (CH), 127.84 (CH), 145.28 (C), 146.68 (C), 147.20 (C), 151.61 (CH), 152.30 (CH). ESI-MS *m/z* 629.2 for [M + Na]⁺. Anal. Calcd for C₃₀H₃₀N₄O₁₀·0.5H₂O: C, 58.53; H, 5.08; N, 9.10. Found: C, 58.57; H, 4.99; N, 8.89.

Synthesis of H₄L³. Pd/C (10%, 20.2 mg) was added to a solution of *trans*-H₄L² (86.3 mg, 0.14 mmol) in dichloromethane/ethanol (1:1, 40 mL), and the mixture was stirred for 30 min at room temperature under 1 atm hydrogen atmosphere. After the catalyst was filtered off and washed with ethanol, the filtrate was concentrated to 1/3 of the original volume. The precipitates were collected to give H₄L³ (51.7 mg, 60%) as colorless crystals; mp 196–198 °C. ¹H NMR (400 MHz, CDCl₃) δ 2.02–2.05 (m, 4H), 4.07–4.10 (m, 4H), 4.45–4.47 (m, 4H), 4.50–4.52 (m, 4H), 6.73 (s, 2H), 6.74 (t, *J* = 7.6 Hz, 2H), 6.78 (dd, *J* = 7.6, 2.0 Hz, 2H), 6.87 (dd, *J* = 7.6, 2.0 Hz, 2H), 8.18 (s, 2H), 8.22 (s, 2H), 9.58 (s, 2H), 9.87 (s, 2H). ¹³C NMR (100 MHz, CDCl₃) δ 26.12 (CH₂), 68.76 (CH₂), 72.83 (CH₂), 75.39 (CH₂), 115.22 (CH), 116.68 (C), 117.65 (C), 119.14 (CH), 121.10 (CH), 122.47 (CH), 145.58 (C), 147.30 (C), 147.47 (C), 151.23 (CH), 152.65 (CH). ESI-MS *m/z* 609.2 for [M + H]⁺. Anal. Calcd for C₃₀H₃₂N₄O₁₀: C, 59.21; H, 5.30; N, 9.21. Found: C, 59.20; H, 5.39; N, 9.01.

Procedure for the Synthesis of [LZn₃(OAc)₂(MeOH)_{*n*}] (L = L¹, *trans*-L², *cis*-L², L³; *n* = 1 or 2). A solution of H₄L in chloroform was mixed with a solution of zinc(II) acetate dihydrate (3.0 equiv) in methanol. The product was precipitated from the reaction mixture (method A) or obtained by recrystallization from chloroform/methanol/ether after removal of the solvent (method B).

[L¹Zn₃(OAc)₂(MeOH)₂]. Yield 73% (method B), yellow crystals. Anal. Calcd for C₃₈H₄₄N₄O₁₆Zn₃·0.5CHCl₃: C, 43.27; H, 4.20; N, 5.24. Found: C, 43.47; H, 4.10; N, 5.57.

[(*trans*-L²)Zn₃(OAc)₂(MeOH)]. Yield 91% (method A), yellow crystals. Anal. Calcd for C₃₅H₃₆N₄O₁₅Zn₃·CHCl₃: C, 40.48; H, 3.49; N, 5.24. Found: C, 40.56; H, 3.68; N, 5.38.

[(*cis*-L²)Zn₃(OAc)₂(MeOH)]. Yield 77% (method A, dichloromethane was used instead of chloroform), yellow crystals. Anal. Calcd for C₃₅H₃₆N₄O₁₅Zn₃·0.5CH₂Cl₂: C, 43.01; H, 3.76; N, 5.65. Found: C, 42.68; H, 3.85; N, 5.69.

[L³Zn₃(OAc)₂(MeOH)]. Yield 80% (method A), yellow crystals. Anal. Calcd for C₃₅H₃₈N₄O₁₅Zn₃·0.5CHCl₃: C, 42.19; H, 3.84; N, 5.54. Found: C, 41.80; H, 3.93; N, 5.65.

Procedure for the Synthesis of [(HL)₂Zn₃(MeOH)₂(H₂O)] (L = *trans*-L², L³). A solution of H₄L (0.0067 mmol) in dichloromethane (33 mL) was mixed with a solution of zinc(II) acetate dihydrate (0.010 mmol) in methanol (33 mL). After the mixture was allowed to stand at room temperature, the precipitates were collected.

[(*trans*-HL²)₂Zn₃(MeOH)₂(H₂O)]. Yield 86%, yellow crystals. Anal. Calcd for C₆₂H₆₄N₈O₂₃Zn₃·CH₂Cl₂: C, 48.18; H, 4.24; N, 7.14. Found: C, 48.63; H, 4.17; N, 7.35.

[(HL³)₂Zn₃(MeOH)₂(H₂O)]. Yield 73%, yellow crystals. Anal. Calcd for C₆₂H₆₈N₈O₂₃Zn₃·0.5CH₂Cl₂: C, 49.00; H, 4.54; N, 7.31. Found: C, 48.90; H, 4.55; N, 7.38.

Procedure for the Synthesis of Heterotrinuclear Complexes. A solution of H₄L (L = L¹, *trans*-L², *cis*-L², L³) in chloroform was mixed with a solution of zinc(II) acetate dihydrate (2 equiv) and metal salt (Ca(OAc)₂·H₂O, Ba(OAc)₂, La(OAc)₃·1.5H₂O) in aqueous methanol. The product was precipitated from the reaction mixture (method A) or obtained by recrystallization from chloroform/methanol/ether after removal of the solvent (method B).

[L¹Zn₂Ca(OAc)₂]. Yield 80% (method B), orange crystals; Anal. Calcd for C₃₆H₃₆CaN₄O₁₄Zn₂·0.5H₂O: C, 46.57; H, 4.02; N, 6.03. Found: C, 46.49; H, 3.99; N, 5.79.

[(*cis*-L²)Zn₂Ca(OAc)₂]. Dichloromethane was used instead of chloroform. Yield 86% (method A), yellow crystals. Anal. Calcd for C₃₄H₃₂CaN₄O₁₄Zn₂: C, 45.81; H, 3.62; N, 6.28. Found: C, 45.92; H, 3.74; N, 6.13.

[L³Zn₂Ca(OAc)₂]. Yield 86% (method A), yellow crystals. Anal. Calcd for C₃₄H₃₄CaN₄O₁₄Zn₂·0.4CHCl₃: C, 43.90; H, 3.68; N, 5.95. Found: C, 43.96; H, 3.82; N, 5.81.

[L¹Zn₂Ba(OAc)₂]. Yield 86% (method B), orange crystals. Anal. Calcd for C₃₆H₃₆BaN₄O₁₄Zn₂·H₂O: C, 41.78; H, 3.70; N, 5.41. Found: C, 41.39; H, 3.76; N, 5.00.

[(*trans*-L²)Zn₂Ba(OAc)₂]. Yield 48% (method A), yellow crystals. Anal. Calcd for C₃₄H₃₂BaN₄O₁₄Zn₂·0.5CHCl₃: C, 39.52; H, 3.12; N, 5.34. Found: C, 39.53; H, 3.46; N, 5.19.

[(*cis*-L²)Zn₂Ba(OAc)₂]. Dichloromethane was used instead of chloroform. Yield 78% (method A), yellow crystals. Anal. Calcd for C₃₄H₃₂BaN₄O₁₄Zn₂·H₂O: C, 40.56; H, 3.40; N, 5.56. Found: C, 40.53; H, 3.47; N, 5.40.

[L³Zn₂Ba(OAc)₂]. Yield 9% (method A), yellow crystals. Anal. Calcd for C₃₄H₃₄BaN₄O₁₄Zn₂·2CHCl₃: C, 35.17; H, 2.95; N, 4.56. Found: C, 35.57; H, 2.98; N, 4.38.

[L¹Zn₂La(OAc)₃]. Yield 88% (method B), orange crystals. Anal. Calcd for C₃₈H₃₉LaN₄O₁₆Zn₂·0.5CHCl₃: C, 40.67; H, 3.50; N, 4.93. Found: C, 40.62; H, 3.79; N, 4.68.

[(*trans*-HL²)Zn₂La(OAc)₄]. Yield 74% (method B), orange crystals. Anal. Calcd for C₃₈H₃₉LaN₄O₁₈Zn₂: C, 41.14; H, 3.54; N, 5.05. Found: C, 41.52; H, 3.82; N, 5.52.

[(*cis*-L²)Zn₂La(OAc)₃]. Yield 78% (method B), orange crystals. Anal. Calcd for C₃₆H₃₅LaN₄O₁₆Zn₂·2H₂O: C, 39.84; H, 3.62; N, 5.16. Found: C, 39.95; H, 3.61; N, 4.97.

[L³Zn₂La(OAc)₃]. Yield 73% (method B), orange crystals. Anal. Calcd for C₃₆H₃₇LaN₄O₁₆Zn₂·1.5CHCl₃·0.5H₂O: C, 36.34; H, 3.21; N, 4.52. Found: C, 36.07; H, 3.17; N, 4.33.

General Procedure of Product Analysis of Ring-Closing Metathesis. A mixture of substrate (H₄L¹, [L¹Zn₃], or [L¹Zn₂M])

Table 1. Crystallographic Data

	<i>trans</i> -H ₄ L ²	<i>cis</i> -H ₄ L ²	[L ¹ Zn ₃ (OAc) ₂ (MeOH) ₂] CHCl ₃ ·0.5MeOH	[(<i>trans</i> -L ²)Zn ₃ (OAc) ₂ (MeOH)] ·0.7CHCl ₃ ·0.5H ₂ O
formula	C ₃₀ H ₃₀ N ₄ O ₁₀	C ₃₀ H ₃₀ N ₄ O ₁₀	C _{39.5} H ₄₇ Cl ₃ N ₄ O _{16.5} Zn ₃	C _{35.7} H _{37.7} Cl _{2.1} N ₄ O _{15.5} Zn ₃
crystal system	triclinic	triclinic	triclinic	monoclinic
space group	<i>P</i> $\bar{1}$	<i>P</i> $\bar{1}$	<i>P</i> $\bar{1}$	<i>P</i> 2 ₁ / <i>n</i>
<i>a</i> /Å	8.4656(13)	9.6197(9)	13.350(6)	10.564(3)
<i>b</i> /Å	20.596(3)	11.0878(10)	14.073(4)	23.317(5)
<i>c</i> /Å	32.583(5)	14.2308(13)	14.187(4)	16.731(5)
α /deg	92.955(2)	81.4800(10)	83.293(12)	
β /deg	90.244(2)	85.2880(10)	68.602(15)	99.821(11)
γ /deg	96.276(2)	73.5460(10)	70.833(14)	
<i>V</i> /Å ³	5639.2(15)	1438.4(2)	2344.0(14)	4060.8(17)
<i>Z</i>	8	2	2	4
<i>T</i> /K	90	100	120	120
<i>D</i> _{calcd} /g cm ⁻³	1.429	1.401	1.621	1.703
<i>R</i> ¹ _a (<i>I</i> > 2 σ (<i>I</i>))	0.0629	0.0387	0.0504	0.0406
<i>wR</i> ² _a (all data)	0.1562	0.0958	0.1551	0.1018
	[(<i>cis</i> -L ²)Zn ₃ (OAc) ₂ (MeOH)] ·0.5CH ₂ Cl ₂	[L ³ Zn ₃ (OAc) ₂ (MeOH)] ·CHCl ₃	[(<i>trans</i> -HL ²) ₂ Zn ₃ (MeOH) ₂ (H ₂ O)] ·6CH ₂ Cl ₂	[(HL ³) ₂ Zn ₃ (MeOH) ₂ (H ₂ O)] ·2.5CH ₂ Cl ₂ ·0.5H ₂ O
formula	C _{35.5} H ₃₇ ClN ₄ O ₁₅ Zn ₃	C ₃₆ H ₃₉ Cl ₃ N ₄ O ₁₅ Zn ₃	C ₆₈ H ₇₆ Cl ₁₂ N ₈ O ₂₃ Zn ₃	C _{64.5} H ₇₄ Cl ₅ N ₈ O _{23.5} Zn ₃
crystal system	monoclinic	monoclinic	triclinic	triclinic
space group	<i>P</i> 2 ₁ / <i>n</i>	<i>P</i> 2 ₁ / <i>n</i>	<i>P</i> $\bar{1}$	<i>P</i> $\bar{1}$
<i>a</i> /Å	10.523(2)	10.630(3)	16.165(6)	13.817(5)
<i>b</i> /Å	23.149(5)	23.876(5)	17.405(5)	15.178(6)
<i>c</i> /Å	16.859(5)	16.861(4)	17.591(5)	18.739(6)
α /deg			97.886(12)	70.992(13)
β /deg	102.788(12)	105.783(11)	110.375(13)	79.984(12)
γ /deg			112.294(13)	85.528(15)
<i>V</i> /Å ³	4004.8(17)	4118.1(18)	4081(2)	3658(2)
<i>Z</i>	4	4	2	2
<i>T</i> /K	120	120	120	120
<i>D</i> _{calcd} /g cm ⁻³	1.644	1.726	1.623	1.553
<i>R</i> ¹ _a (<i>I</i> > 2 σ (<i>I</i>))	0.0727	0.0484	0.0992	0.0722
<i>wR</i> ² _a (all data)	0.2063	0.1422	0.2553	0.1675
	[L ¹ Zn ₂ Ca(OAc) ₂]·0.5CHCl ₃ · 0.5MeOH		[(<i>cis</i> -L ²)Zn ₂ Ca(OAc) ₂]· 1.5CH ₂ Cl ₂	[L ³ Zn ₂ Ca(OAc) ₂]· 2CHCl ₃
formula	C ₃₇ H _{38.5} CaCl _{1.5} N ₄ O _{14.5} Zn ₂		C _{35.5} H ₃₅ CaCl ₃ N ₄ O ₁₄ Zn ₂	C ₃₆ H ₃₆ CaCl ₆ N ₄ O ₁₄ Zn ₂
crystal system	triclinic		triclinic	triclinic
space group	<i>P</i> $\bar{1}$		<i>P</i> $\bar{1}$	<i>P</i> $\bar{1}$
<i>a</i> /Å	13.791(3)		11.826(6)	13.129(5)
<i>b</i> /Å	15.788(4)		12.942(5)	13.629(5)
<i>c</i> /Å	20.439(4)		14.995(7)	14.925(8)
α /deg	84.018(10)		63.850(13)	76.252(15)
β /deg	81.632(10)		71.662(18)	66.462(15)
γ /deg	73.877(11)		82.025(17)	62.042(12)
<i>V</i> /Å ³	4220.1(17)		1955.6(15)	2158.4(16)
<i>Z</i>	4		2	2
<i>T</i> /K	120		120	120
<i>D</i> _{calcd} /g cm ⁻³	1.566		1.730	1.742
<i>R</i> ¹ _a (<i>I</i> > 2 σ (<i>I</i>))	0.0638		0.0523	0.0567
<i>wR</i> ² _a (all data)	0.1839		0.1335	0.1530
	[L ¹ Zn ₂ Ba(OAc) ₂]· 0.7CHCl ₃ ·0.6MeOH	[(<i>trans</i> -L ²)Zn ₂ Ba(OAc) ₂]· 1.5CHCl ₃ ·0.5Et ₂ O	[(<i>cis</i> -L ²)Zn ₂ Ba(OAc) ₂]· 0.5MeOH	[L ³ Zn ₂ Ba(OAc) ₂]· 2CHCl ₃
formula	C _{37.3} H _{39.1} BaCl _{2.1} N ₄ O _{14.6} Zn ₂	C _{37.5} H _{38.5} BaCl _{4.5} N ₄ O _{14.5} Zn ₂	C _{34.5} H ₃₄ Ba ₄ N ₄ O _{14.5} Zn ₂	C ₃₆ H ₃₆ BaCl ₆ N ₄ O ₁₄ Zn ₂
crystal system	triclinic	triclinic	triclinic	triclinic
space group	<i>P</i> $\bar{1}$	<i>P</i> $\bar{1}$	<i>P</i> $\bar{1}$	<i>P</i> $\bar{1}$
<i>a</i> /Å	14.446(4)	12.580(6)	10.5880(6)	12.715(5)
<i>b</i> /Å	15.882(3)	13.505(5)	13.0232(7)	13.474(6)
<i>c</i> /Å	20.178(6)	15.324(7)	15.2344(8)	15.258(8)
α /deg	88.392(9)	79.997(14)	103.5402(16)	79.705(18)
β /deg	79.764(11)	70.491(17)	107.7635(15)	69.719(17)
γ /deg	69.993(8)	65.950(16)	102.6695(17)	65.578(14)
<i>V</i> /Å ³	4278.1(18)	2238.7(17)	1846.52(17)	2230.6(17)
<i>Z</i>	4	2	2	2
<i>T</i> /K	120	120	120	120
<i>D</i> _{calcd} /g cm ⁻³	1.738	1.787	1.807	1.831
<i>R</i> ¹ _a (<i>I</i> > 2 σ (<i>I</i>))	0.0354	0.0402	0.0398	0.0350
<i>wR</i> ² _a (all data)	0.0953	0.1021	0.1105	0.0879

Table 1. Continued

	[L ¹ Zn ₂ La(OAc) ₃]·CHCl ₃	[(<i>trans</i> -HL ²)Zn ₂ La(OAc) ₄ (H ₂ O)]	[(<i>cis</i> -L ²)Zn ₂ La(OAc) ₃ (MeOH) _{0.75}]·1.5MeOH	[L ³ Zn ₂ La(OAc) ₃ (MeOH) _{0.5}]·1.5CHCl ₃
formula	C ₃₉ H ₄₀ Cl ₃ LaN ₄ O ₁₆ Zn ₂	C ₃₈ H ₄₁ LaN ₄ O ₁₉ Zn ₂	C _{38.25} H ₄₄ LaN ₄ O _{18.25} Zn ₂	C ₃₈ H _{40.5} Cl _{4.5} LaN ₄ O _{16.5} Zn ₂
crystal system	triclinic	triclinic	triclinic	triclinic
space group	<i>P</i> $\bar{1}$	<i>P</i> $\bar{1}$	<i>P</i> $\bar{1}$	<i>P</i> $\bar{1}$
<i>a</i> /Å	12.836(5)	14.002(4)	12.515(5)	12.504(5)
<i>b</i> /Å	13.302(5)	18.183(6)	13.342(6)	13.294(6)
<i>c</i> /Å	14.564(5)	18.530(5)	13.551(6)	15.402(5)
α /deg	115.026(14)	69.979(11)	109.182(17)	88.589(15)
β /deg	94.160(17)	86.008(10)	94.939(17)	80.960(13)
γ /deg	93.458(17)	73.150(12)	91.653(16)	65.885(15)
<i>V</i> /Å ³	2236.0(14)	4240(2)	2125.3(16)	2305.6(15)
<i>Z</i>	2	4	2	2
<i>T</i> /K	120	120	120	120
<i>D</i> _{calcd} /g cm ⁻³	1.778	1.766	1.752	1.795
<i>R</i> ^a (<i>I</i> > 2 σ (<i>I</i>))	0.0468	0.0535	0.0341	0.0619
<i>wR</i> ^a (all data)	0.1408	0.1500	0.0868	0.1591

$$^a R1 = \sum ||F_o| - |F_c|| / \sum |F_o|; wR2 = [\sum w(F_o^2 - F_c^2)^2 / \sum w(F_o^2)^2]^{1/2}.$$

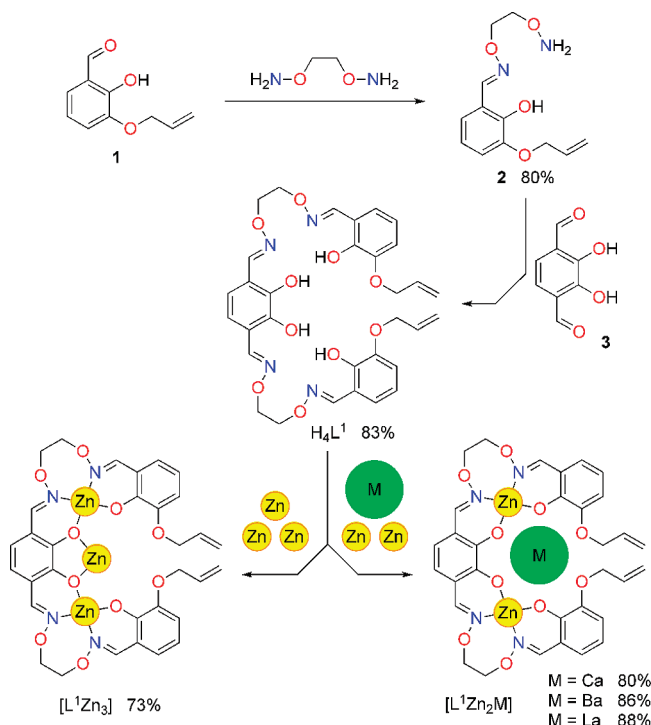
(0.020 mmol), catalyst (Grubbs I or II), and solvent was stirred in the dark under argon atmosphere under the conditions A (in dichloromethane, 1 mM, RT, 30 h) or B (in THF, 5 mM, reflux, 9 h). The solvent was then removed under reduced pressure. When metal complex was used as the substrate, chloroform and 1 M hydrochloric acid were added to the mixture, which was stirred for 1 h at room temperature, and then the organic layer was separated, dried over anhydrous magnesium sulfate, and concentrated to dryness. The mixture was analyzed by ¹H NMR (CDCl₃) and GPC.

Characterization of Byproducts 4 and 5. **4:** ¹H NMR (400 MHz, CDCl₃) δ 4.47–4.52 (m, 8H), 4.63 (d, *J* = 5.3 Hz, 2H), 5.29 (dd, *J* = 10.6, 1.4 Hz, 1H), 5.42 (dd, *J* = 17.2, 1.4 Hz, 1H), 5.61 (brs, 1H), 6.10 (ddt, *J* = 17.2, 10.6, 5.3 Hz, 1H), 6.74 (dd, *J* = 7.8, 1.5 Hz, 1H), 6.77 (s, 2H), 6.80–6.85 (m, 3H), 6.92 (dd, *J* = 6.9, 2.7 Hz, 1H), 6.96 (dd, *J* = 7.8, 1.5 Hz, 1H), 8.22 (s, 1H), 8.23 (s, 1H), 8.24 (s, 1H), 8.26 (s, 1H), 9.61 (s, 1H), 9.70 (s, 1H), 9.73 (s, 1H), 9.92 (s, 1H). **5:** ¹H NMR (400 MHz, CDCl₃) δ 4.50–4.52 (m, 8H), 5.61 (brs, 2H), 6.74 (dd, *J* = 7.9, 1.1 Hz, 2H), 6.78 (s, 2H), 6.82 (t, *J* = 7.9 Hz, 2H), 6.96 (dd, *J* = 7.9, 1.1 Hz, 2H), 8.22 (s, 2H), 8.23 (s, 2H), 9.66 (s, 2H), 9.92 (s, 2H).

¹H NMR Titration (Ligand-Zinc(II)). Sample solutions containing ligand (1.0 mM for H₄L¹; 0.5 mM for *trans*-H₄L², *cis*-H₄L², H₄L³) and varying amount of zinc(II) acetate dihydrate (0 to 5 equiv) in CDCl₃/CD₃OD (1:1, 0.6 mL) were prepared. ¹H NMR spectrum (400 MHz) of each sample was recorded at 298 K.

¹H NMR Titration (Ligand-Zinc(II)-Guest Cation). Sample solutions containing ligand (H₄L¹, *trans*-H₄L², *cis*-H₄L², H₄L³; 0.5 mM), zinc(II) acetate dihydrate (1.5 mM), and guest cation (La(NO₃)₃ or M(OAc)₂ (M = Mg, Ca, Ba); 0 to 3 equiv) in CDCl₃/CD₃OD (1:1, 0.6 mL) were prepared. ¹H NMR spectra (400 MHz) were recorded at 298 K.

X-ray Crystallographic Analysis. Intensity data were collected on a Rigaku R-Axis Rapid or a Bruker SMART APEX II diffractometer with Mo K α radiation (λ = 0.71069 Å). The data were corrected for Lorentz and polarization factors, and for absorption by semiempirical methods based on symmetry-equivalent and

Scheme 2. Synthesis of Ligand H₄L¹ and Its Metal Complexes

repeated reflections. The structures were solved by direct methods (SIR97)¹³ or Patterson methods (DIRDIF 99)¹⁴ and refined by full-matrix least-squares on *F*² using SHELXL 97.¹⁵ The crystallographic data are summarized in Table 1.

Results and Discussion

Synthesis of Ligand H₄L¹ and Its Metal Complexes. The diallyl ligand H₄L¹ was synthesized by a procedure analogous to that for the corresponding methoxy derivative (Scheme 2)¹⁰ as described in the preliminary communication.⁹ The reaction of 3-allyloxy-2-hydroxybenzaldehyde (1)¹¹ with excess 1,2-bis(aminoxy)ethane¹² afforded the

(13) SIR97, program for crystal structure solution: Altomare, A.; Burla, M. C.; Camalli, M.; Cascarano, G. L.; Giacovazzo, C.; Guagliardi, A.; Moliterni, A. G. G.; Polidori, G.; Spagna, R. *J. Appl. Crystallogr.* **1999**, *32*, 115–119.

(14) Beurskens, P. T.; Beurskens, G.; de Gelder, R.; Garcia-Granda, S.; Gould, R. O.; Israel, R.; Smits, J. M. M. *The DIRDIF-99 Program system*; Crystallography Laboratory, University of Nijmegen: Nijmegen, The Netherlands, 1999.

(15) Sheldrick, G. M. *SHELXL 97, Program for crystal structure refinement*; University of Göttingen: Göttingen, Germany, 1997.

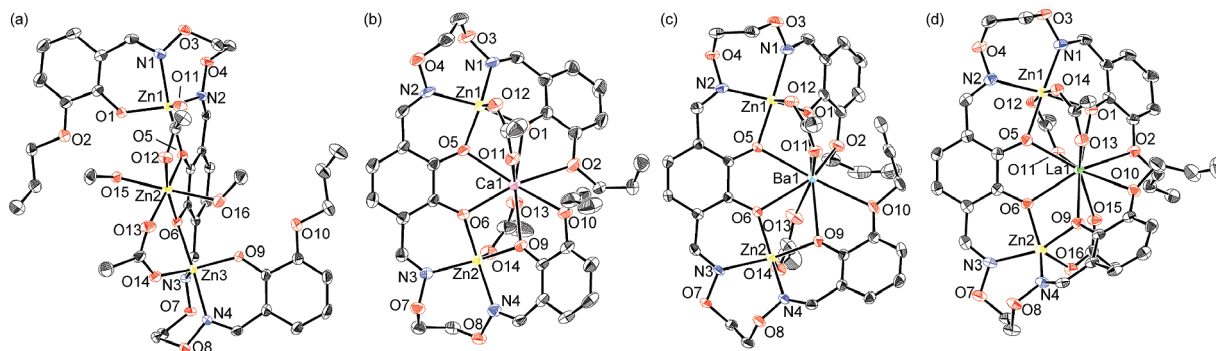


Figure 1. X-ray crystal structures of the trinuclear complexes (a) $[L^1Zn_3(OAc)_2(MeOH)_2]$, (b) $[L^1Zn_2Ca(OAc)_2]$, (c) $[L^1Zn_2Ba(OAc)_2]$, and (d) $[L^1Zn_2La(OAc)_3]$ with thermal ellipsoids drawn at 50% probability level. Hydrogen atoms, disordered atoms, and solvent molecules are omitted for clarity. One of the crystallographically independent molecules is shown for $[L^1Zn_2Ca(OAc)_2]$ and $[L^1Zn_2Ba(OAc)_2]$.

oxime **2** in 80% yield. The target H_4L^1 ligand was obtained in 83% yield by the reaction of **2** with 2,3-dihydroxybenzene-1,4-dicarbaldehyde (**3**)^{10c} in ethanol.

The corresponding metal complexes were prepared by the reaction with the appropriate metal salts according to the reported procedure.⁹ The complexation of H_4L^1 with 3 equiv of zinc(II) acetate produced the homotrimeric complex $[L^1Zn_3]$ in 73% yield. Heterotrimeric complexes $[L^1Zn_2Ca]$, $[L^1Zn_2Ba]$, and $[L^1Zn_2La]$ were obtained by the reaction of H_4L^1 with 2 equiv of zinc(II) acetate and 1 equiv of the central metal source, $Ca(OAc)_2$, $Ba(OAc)_2$, and $La(OAc)_3$, respectively, in 80–88% yields.

Structure of Metal Complexes. The structures of the complexes were determined by X-ray crystallography. The structures of $[L^1Zn_3]$, $[L^1Zn_2Ca]$, and $[L^1Zn_2La]$ were already reported in the preliminary communication,⁹ and we here report the structure of $[L^1Zn_2Ba]$ to investigate the effect of the ionic radius of the central metal ions.

The homotrimeric complex $[L^1Zn_3]$ adopts an S-shaped conformation in which the two terminal allyl groups point in opposite directions (Figure 1a). The distance between the two allylic carbons (d_{CC}) is 12.3 Å (Table 2). Neither the allyloxy (O2 and O10) nor phenoxo groups (O1 and O9) coordinate to Zn2 in the central O_6 site. The coordination geometry of the central zinc (Zn2) is a distorted octahedral, two from the catechol moiety of ligand L^{4-} , two from μ -acetato, and two from methanol molecules. Such a structural feature is in striking contrast to the conformation of the methoxy analogue,^{10a,c} in which two methoxy groups are close to each other (the C–C distance between the methoxy groups is 3.724 Å). Thus, the molecular shape of the $[L^1Zn_3]$ complex is sensitive to the slight difference in the terminal alkyl group.¹⁶

For the heterotrimeric complexes, all four phenoxo oxygen donors and allyloxy groups coordinate to the central metal cation (Ca, Ba, La) at the central O_6 site (Figure 1b–d). The coordination makes the acyclic ligand L^1 wrap around the central metal cation in a C-shaped helical fashion. The distances between the two terminal allylic carbons are much less shorter ($d_{CC} = 3.2$ – 5.8 Å) compared to that of $[L^1Zn_3]$. The winding angle of $[L^1Zn_2Ba]$ ($\theta = 290$ – 294°) is considerably smaller than

Table 2. Geometrical Features of the Metal Complexes of Diallyl Ligand H_4L^1

complex	distance (Å)			winding angle
	d_{CC}^a	d_{OO}^b	d_{MO}^c	θ (deg) ^d
$[L^1Zn_3]$	12.312	10.121	(3.749) ^e	— ^g
$[L^1Zn_2Ca]$	(A) ^e 3.933, 4.160 ^f	3.150	2.496	314.8
	(B) ^e 3.754, 3.626 ^f	3.093	2.469	319.7
$[L^1Zn_2Ba]$	(A) ^e 5.771, 4.924 ^f	4.360	2.747	293.8
	(B) ^e 5.067, 5.431 ^f	4.443	2.761	290.5
$[L^1Zn_2La]$	3.903	3.361	2.583	315.8

^a Defined as the distance between the two allylic carbon atoms.

^b Defined as the distance between the two allyloxy oxygen atoms.

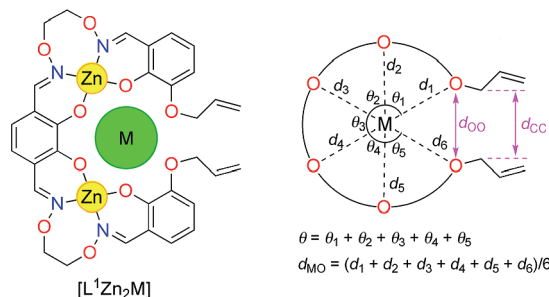
^c Defined as the average of the six M–O distances d_1 – d_6 .

^d Defined as the sum of the five O–M–O angles θ_1 – θ_5 .

^e A and B denote the crystallographically independent molecules.

^f The allyl groups are disordered over two positions.

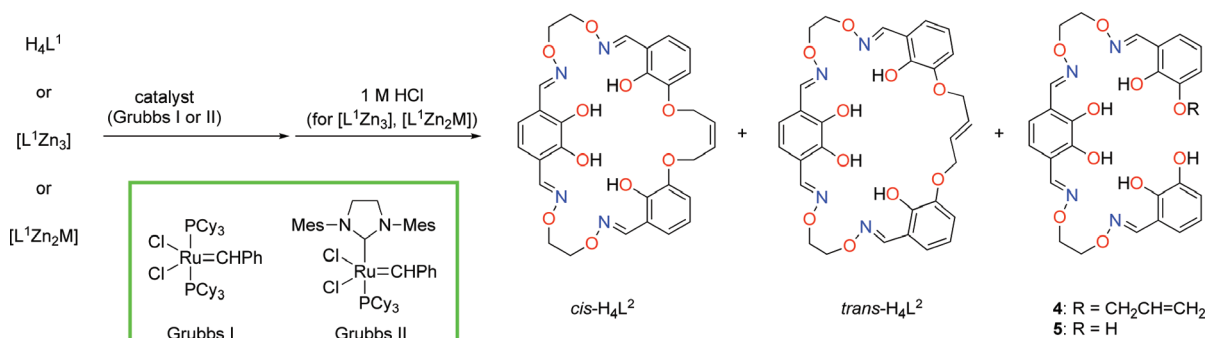
^g Non helical, S-shaped conformation in which some oxygen atoms do not coordinate to M.



those of the lanthanum and calcium complexes ($\theta = 315$ – 320°) because of the longer Ba–O distances (average Ba–O distances, 2.75 Å; Ca–O, 2.48 Å; La–O, 2.58 Å).

Conversion to the Three Kinds of Cyclic Ligands. Ring-closing metathesis of the diallyl ligand H_4L^1 and its metal complexes was carried out to obtain the corresponding macrocyclic compounds (Scheme 3), some of which are reported in the preliminary communication.⁹ Treatment of the free ligand H_4L^1 in dichloromethane (1 mM) with Grubbs I catalyst afforded the corresponding monomeric macrocycle H_4L^2 in addition to a small amount of oligomeric products. The crude product contained the *cis* and *trans* isomers of H_4L^2 (Table 3, entry 1) in a 7:93 ratio. The major product, that is, the *trans* isomer, can be easily isolated in 68% yield by recrystallization of the crude product. The X-ray crystallographic analysis of the major isomer unambiguously determined the *trans* configuration of the olefinic moiety, as well as the monomeric macrocyclic structure (Figure 2a). In the crystal

(16) Akine, S.; Taniguchi, T.; Nabeshima, T. *Inorg. Chem.* **2008**, *47*, 3255–3264.

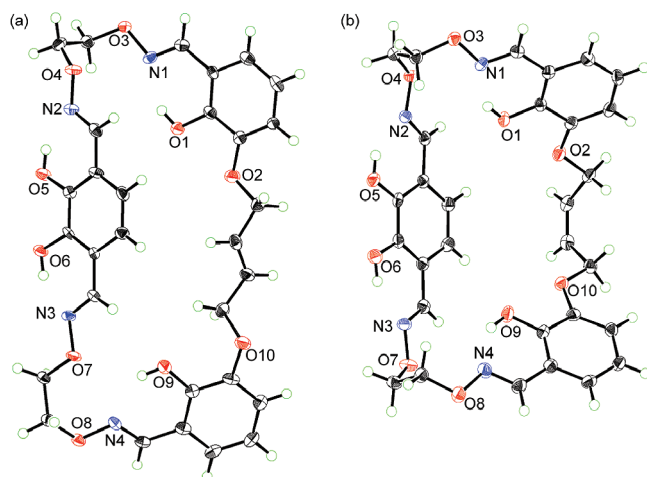
Scheme 3. Ring-Closing Metathesis of H_4L^1 and Its Metal Complexes**Table 3.** Ring-Closing Metathesis of H_4L^1 and Its Metal Complexes^a

entry	substrate	catalyst mol %	conditions ^b	yield (%)				H_4L^1 recovery
				H_4L^2	$cis/trans^c$	4	5	
1	H_4L^1	I, 5	A	94 ^d [68, <i>trans</i>]	7:93	0	0	0
2	H_4L^1	II, 10	A	89 ^d	6:94	0	0	7
3	$[L^1Zn_3]$	I, 10	B	13	25:75	19	0	63
4	$[L^1Zn_3]$	II, 10	B	58	32:68	12	4	16
5	$[L^1Zn_2Ca]$	II, 10	B	77 [64, <i>cis</i>]	100:0	4	0	16
6	$[L^1Zn_2Ba]$	II, 10	B	73	24:76	0	0	17
7	$[L^1Zn_2La]$	II, 10	B	5	100:0	58	5	26

^a Yields were determined from 1H NMR spectra of the crude reaction mixture. Isolated yields after recrystallization are given in brackets.

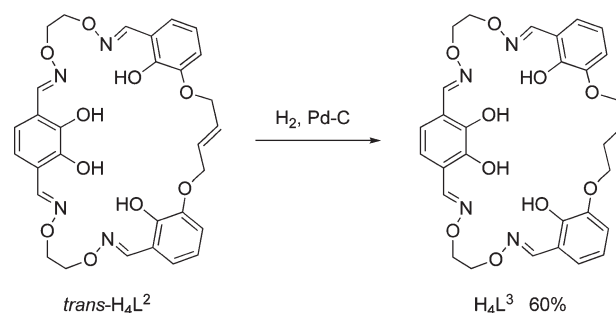
^b A: In dichloromethane, 1 mM, RT, 30 h. B: In THF, 5 mM, reflux, 9 h, followed by demetalation with 1 M HCl. ^c *Cis/trans* ratios of macrocycle H_4L^2 .

^d The product contains a small amount of oligomeric compounds.

**Figure 2.** Crystal structures of (a) $trans-H_4L^2$ (one of the crystallographically independent molecules is shown) and (b) $cis-H_4L^2$ with thermal ellipsoids drawn at 50% probability level.

structure, there are $O-H \cdots N$ hydrogen bonds in the salicylaldoxime moieties with the $O-N$ distances ranging from 2.59 to 2.71 Å. These hydrogen bonds are probably responsible for the relatively high yield of the monomeric 32-membered macrocycle without using a template metal, because the intramolecular hydrogen bonds significantly reduce the conformational flexibility during the cyclization reaction. Use of Grubbs II instead of Grubbs I did not significantly change the product ratio (entry 2).

In contrast, the metathesis reaction of $[L^1Zn_3]$ with Grubbs I did not efficiently proceed (entry 3). The reaction with Grubbs II gave the cyclic product H_4L^2 in a better yield (entry 4) after demetalation with dilute

Scheme 4. Synthesis of Saturated Ligand H_4L^3 

hydrochloric acid. It is noteworthy that the *cis/trans* ratio of the cyclic product H_4L^2 significantly changed in the case of the zinc(II) complex (32:68).

The reaction of $[L^1Zn_2Ca]$ mainly gave the *cis* cyclic product (entry 5). Pure *cis*- H_4L^2 was isolated in 64% yield after recrystallization of the crude product (Figure 2b). The selectivity dramatically changed in the case of $[L^1Zn_2Ba]$ (entry 6); the *trans* isomer was the major product (*cis/trans* = 24:76). The reaction of $[L^1Zn_2La]$ afforded only the *cis*- H_4L^2 as a cyclic product in lower yield (entry 7). Instead, the deallylated products 4 and 5 were formed (Scheme 3). Consequently, the metal ions M in the substrates $[L^1Zn_2M]$ significantly affect the yield and *cis/trans* selectivity of the ring closing metathesis.¹⁷

As a result, *cis*- H_4L^2 was very efficiently obtained from $[L^1Zn_2Ca]$ after demetalation, and *trans*- H_4L^2 was obtained from the free ligand H_4L^1 . Pure samples of the

(17) (a) Marsella, M. J.; Maynard, H. D.; Grubbs, R. H. *Angew. Chem., Int. Ed. Engl.* **1997**, 36, 1101–1103. (b) König, B.; Horn, C. *Synlett* **1996**, 1013–1014.

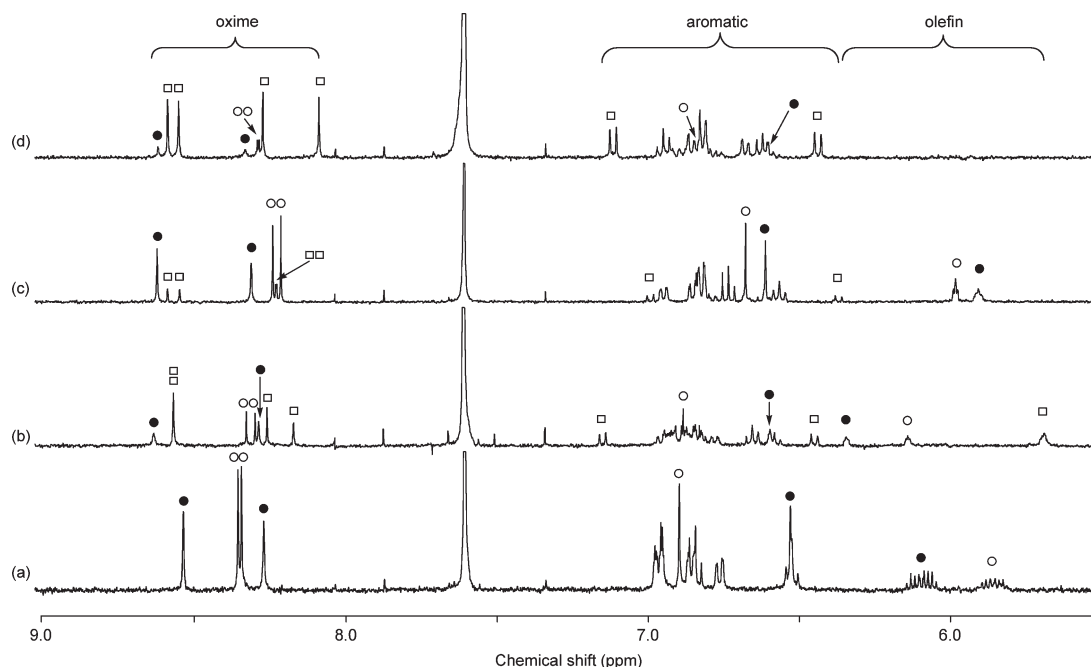


Figure 3. ^1H NMR spectra of H_4L ((a) $\text{L} = \text{L}^1$; (b) $\text{L} = \text{trans-L}^2$; (c) $\text{L} = \text{cis-L}^2$; (d) $\text{L} = \text{L}^3$) in the presence of 1.5 equiv of zinc(II) acetate (400 MHz, $\text{CDCl}_3/\text{CD}_3\text{OD}$, 1:1, 0.5 mM). Filled circles, open circles, and open squares denote H_4L , $[\text{LZn}_3]$, and $[(\text{HL})_2\text{Zn}_3]$, respectively. The oxime protons, aromatic protons of catecholato moiety, and olefinic protons are marked in the spectra.

cis and *trans* isomers for the complexation study (see below) were prepared by these methods. The saturated ligand H_4L^3 was prepared by the hydrogenation of *trans*- H_4L^2 using the Pd/C catalyst (Scheme 4).

Complexation with Zinc(II). We have previously reported that the methoxy substituted ligand forms a trinuclear complex with zinc(II) and that the complexation process is highly cooperative.¹⁰ The allyloxy substituted derivative, H_4L^1 , formed a similar homotrimeric complex $[\text{L}^1\text{Zn}_3]$ in a highly cooperative fashion as observed for those of the methoxy derivative. When 1.5 equiv of zinc(II) ion was added, half of the ligand H_4L^1 was converted into the trinuclear complex $[\text{L}^1\text{Zn}_3]$, and the other half remained unchanged (Figure 3a).

The trinuclear complexes $[\text{LZn}_3]$ ($\text{L} = \text{trans-L}^2$, *cis*- L^2 , L^3) were almost quantitatively formed upon the addition of 3 equiv of zinc(II) acetate. The structures of these trinuclear complexes were determined by X-ray crystallography (Figure 4a–c). In these complexes, the zinc(II) trinuclear core is bridged by acetato ligands as observed in the methoxy analogue.^{10a,c}

However, when less than 3 equiv of zinc(II) acetate was added, the ^1H NMR spectra of the cyclic ligands H_4L ($\text{L} = \text{trans-L}^2$, *cis*- L^2 , L^3) showed signals other than those of H_4L and $[\text{LZn}_3]$. These signals are assignable to an intermediate species during the formation process of the trinuclear complex $[\text{LZn}_3]$. The mole fraction of the intermediate species was at the maximum when 1.5 equiv of zinc(II) acetate was added (Figure 3b–d). This indicates that the intermediate complex has a 2:3 (ligand/metal) stoichiometry. The maximum mole fractions of the intermediate complexes were 53% (*trans*- L^2 ; Figure 3b), 17% (*cis*- L^2 ; Figure 3c), and 76% (L^3 ; Figure 3d).

From a solution of *trans*- H_4L^2 or H_4L^3 containing 1.5 equiv of zinc(II) acetate, yellow crystals of the intermediate complexes were isolated. The crystallographic study

revealed that the intermediate was the 2:3 complex $[(\text{HL})_2\text{Zn}_3]$ ($\text{L} = \text{trans-L}^2$, L^3) (Figure 4d, e). These complexes consist of two molecules of the triply deprotonated ligand $(\text{HL})^{3-}$ and three zinc(II) ions. Two $[(\text{HL})\text{Zn}]$ units are held together by the third zinc(II) ion via the coordination of the catecholato moiety of each $[(\text{HL})\text{Zn}]$ unit. In the $[(\text{HL})\text{Zn}]$ unit, the two N_2O_2 coordination moieties (salamo moieties, hereafter) are in a nonequivalent environment; one of the two salamo moieties is metalated while the other is vacant.

This unsymmetrical feature is also evident in solution. The ^1H NMR spectra of the intermediates exhibit four singlets with equal intensities for the oxime protons (8.0–8.6 ppm). In addition, a pair of doublets was observed for the aromatic protons of the central catecholato moiety (Figure 3b–d; signals marked by open squares at 6.4–7.2 ppm). These spectral patterns are consistent with the crystal structures, in which the two salamo moieties are in nonequivalent environments. The formation of the 2:3 complex was also confirmed by the peak at m/z 1403.1 for $[(\text{trans-HL}^2)_2\text{Zn}_3 + \text{H}]^+$ in the ESI-MS measurements.

Consequently, the complexation of the cyclic ligands H_4L ($\text{L} = \text{trans-L}^2$, *cis*- L^2 , L^3) with zinc(II) acetate gave the trinuclear complex $[\text{LZn}_3]$ in a non-cooperative, stepwise fashion via the intermediate 2:3 complex $[(\text{HL})_2\text{Zn}_3]$, whereas the formation of the acyclic analogue $[\text{L}^1\text{Zn}_3]$ was cooperative. The conversion of H_4L^1 into cyclic ligands significantly changes the formation process of the trinuclear complexes $[(\text{HL})_2\text{Zn}_3]$ and $[\text{LZn}_3]$ (Scheme 5).

Selectivity in Guest Ion Recognition via the Metal Exchange of Zinc(II) Trinuclear Complexes. We have previously reported that the zinc(II) homotrimeric complex having methyl groups instead of the olefinic moieties can recognize guest ions by the site-selective

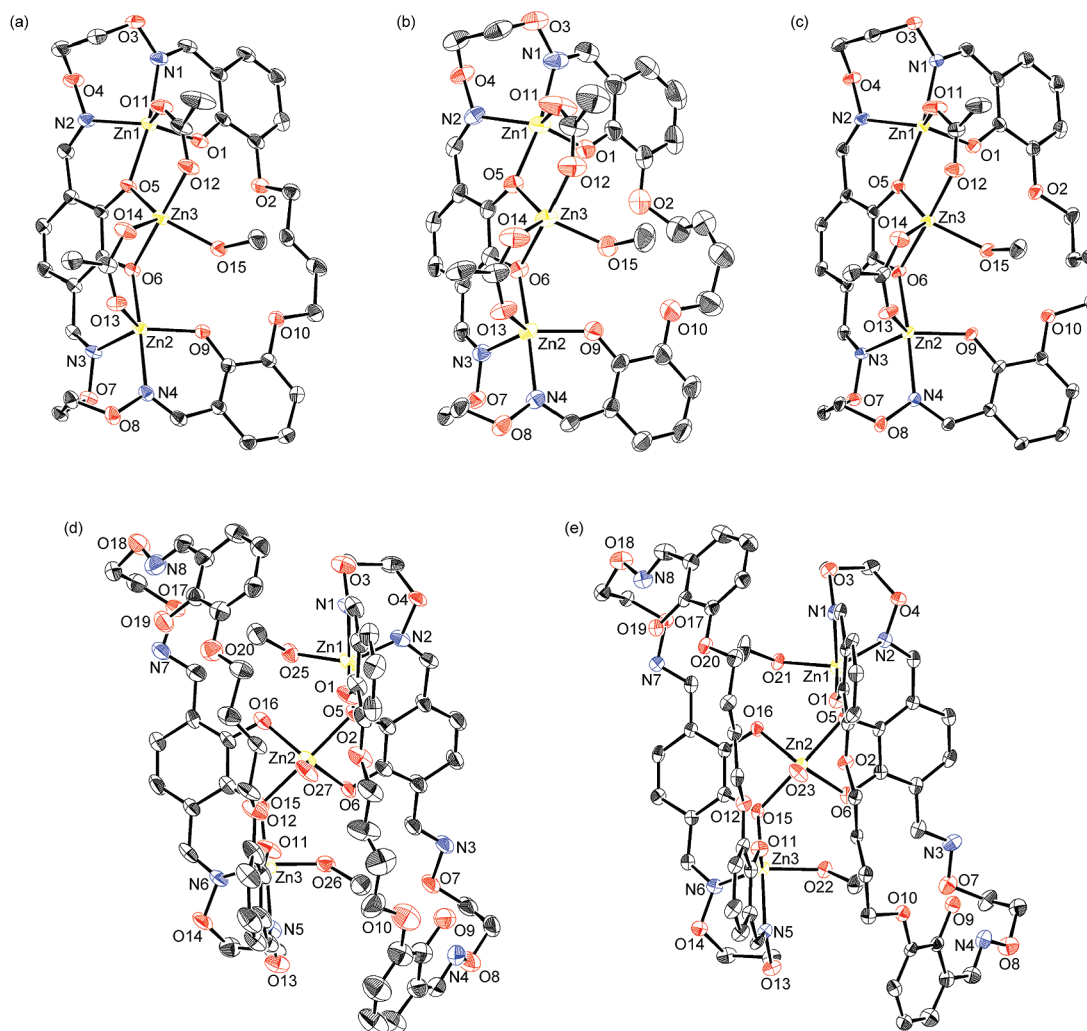
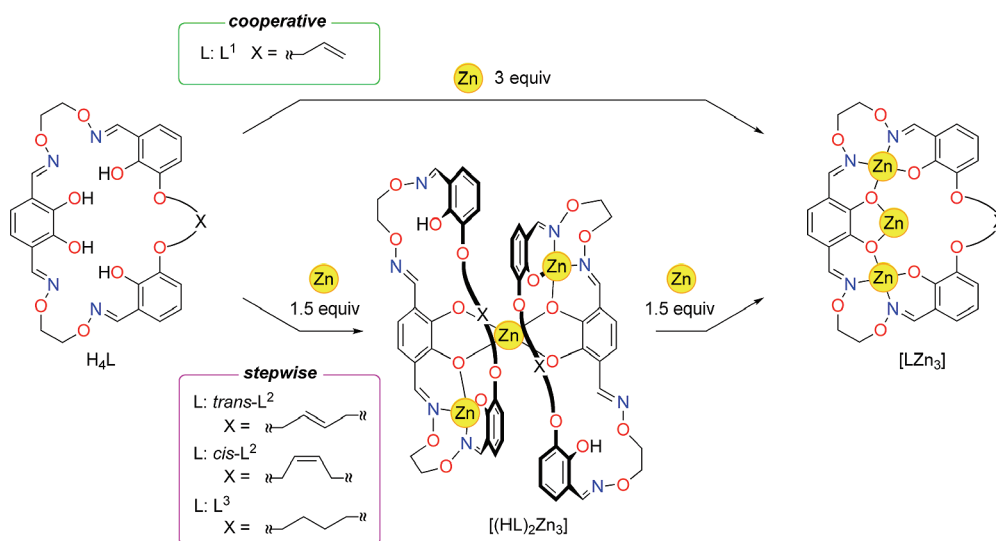


Figure 4. X-ray structures of (a) $[(trans-L^2)Zn_3(OAc)_2(MeOH)]$, (b) $[(cis-L^2)Zn_3(OAc)_2(MeOH)]$, (c) $[L^3Zn_3(OAc)_2(MeOH)]$, (d) $[(trans-HL^2)_2Zn_3(MeOH)_2(H_2O)]$, and (e) $[(HL^3)_2Zn_3(MeOH)_2(H_2O)]$ with thermal ellipsoids drawn at 50% (a, b, c) or 30% (d, e) probability level. Hydrogen atoms, disordered atoms, and solvent molecules are omitted for clarity.

Scheme 5. Complexation of Acyclic Ligand (H_4L^1) and Cyclic Ligands ($trans-H_4L^2$, $cis-H_4L^2$, H_4L^3) with Zinc(II) Acetate



metal exchange.¹⁰ The metal exchange efficiently proceeds upon the addition of rare earth metals and Ca^{2+} . The guest ion recognition behavior of the trinuclear complexes $[LZn_3]$

($L = L^1, trans-L^2, cis-L^2, L^3$) is studied to clarify the ring effects and the structural effects of the linking moiety between the salamo moieties (Scheme 6, Table 4).

As expected, four complexes $[LZn_3]$ ($L = L^1$, *trans*- L^2 , *cis*- L^2 , L^3) showed a different selectivity in the recognition of alkaline earth metal ions. The acyclic derivative $[L^1Zn_3]$ showed Ca^{2+} selectivity, as observed for the methoxy derivative.^{10b,e} Although the crystal structures of $[L^1Zn_3]$ and the methoxy derivative were significantly different from each other, the structural fluxionality in solution probably leads to the similar complexation behavior. On the contrary, $[(trans-L^2)Zn_3]$ binds Ba^{2+} much stronger than Ca^{2+} or Mg^{2+} . Thus, the Ca^{2+}/Ba^{2+} selectivity is reversed from 13 to 1/300 by the conversion of the acyclic L^1 to the *trans*- L^2 . This probably results from the restricted conformation of the cyclic ligand *trans*- H_4L^2 compared to the corresponding acyclic derivative H_4L^1 . The longer *trans*-olefin linkage fixes the two ether oxygen atoms further apart from each other. This makes the cavity large enough to surround larger cations such as Ba^{2+} .

The shorter *cis*-olefin linkage has a different effect on the metal exchange equilibrium. As expected, the metal exchange of $[(cis-L^2)Zn_3]$ with Ca^{2+} very efficiently took place. The $[(cis-L^2)Zn_3]$ can also recognize Ba^{2+} despite its larger ionic radius than the cavity size. In this case, the guest sits at a position displaced from the center of the cavity keeping suitable O–Ba distances from the oxygen donor atoms. The equilibrium constants of $[(cis-L^2)Zn_3]$ with Ca^{2+} and Ba^{2+} are higher than that of the acyclic derivative $[L^1Zn_3]$. On the other hand, the metal exchange of $[(cis-L^2)Zn_3]$ with Mg^{2+} was less efficient than that of $[L^1Zn_3]$. This is presumably attributed to the conformational constraint of the macrocycle that prevents all of the six oxygen donor atoms from coordinating to the small Mg^{2+} . Consequently, the Ca^{2+}/Mg^{2+} or Ba^{2+}/Mg^{2+} selectivity significantly increased after the conversion of L^1 to *cis*- L^2 .

The saturated analogue $[L^3Zn_3]$ exhibited a binding behavior similar to that of $[(cis-L^2)Zn_3]$. This result is rationalized by the flexible tetramethylene linker that would change its conformation suitable for the guest recognition.

When La^{3+} was used as a guest, the metal exchange of the central Zn^{2+} with La^{3+} quantitatively proceeded regardless of the ligand structure (L^1 , *trans*- L^2 , *cis*- L^2 , L^3). This is probably because the binding of the phenoxo moieties to La^{3+} via an electrostatic interaction is stronger than that to the divalent cations (Ca^{2+} and Ba^{2+}). The stabilization must be high enough to replace the Zn^{2+} in the central cavity, even though La^{3+} does not always fit well into the central O_6 cavity.

Crystal Structures of Metallohost–Guest Complexes.

X-ray crystallographic analysis was carried out to investigate the structure in relation to the stability of the metallohost–guest complexes. In the crystal structure of $[(cis-L^2)Zn_2Ca(OAc)_2]$, all the six oxygen donor atoms of the recognition site coordinate to Ca^{2+} (Figure 5a). The distance between the two allyloxy oxygen atoms (d_{OO}) is 2.8 Å (Table 5), which is slightly shorter than that of the acyclic analogue $[L^1Zn_2Ca(OAc)_2]$ ($d_{OO} = 3.1$ Å). This structural resemblance indicates that the *cis*-olefin linkage does not produce a significant strain in the Zn_2Ca trinuclear moiety. This is the reason why the metal exchange of $[(cis-L^2)Zn_3]$ by calcium ion efficiently occurred. The structural resemblance also accounts for the high efficiency of the ring-closure and excellent *cis/trans* selectivity of $[L^1Zn_2Ca]$, because the olefin metathesis giving the *cis* olefin is expected to proceed without any large structural deformations. The saturated analogue $[L^3Zn_2Ca(OAc)_2]$ adopted a similar structure with $d_{OO} = 2.9$ Å (Figure 5b), in which the tetramethylene moiety adopted a *gauche* conformation to make a cavity size suitable for Ca^{2+} . Crystals of $[(trans-L^2)Zn_2Ca(OAc)_2]$ were not obtained probably because of the low efficiency of the metal exchange (equilibrium constant $K = 0.20$).

In the case of barium complexes, single crystals of $[LZn_2Ba(OAc)_2]$ were obtained for all the three cyclic ligands ($L = trans-L^2$, *cis*- L^2 , L^3). These three complexes have a similar structure in which the six oxygen donor atoms coordinated to the barium ion in the central O_6 site

Scheme 6. Ion Recognition by Trinuclear Complexes Based on Metal Exchange

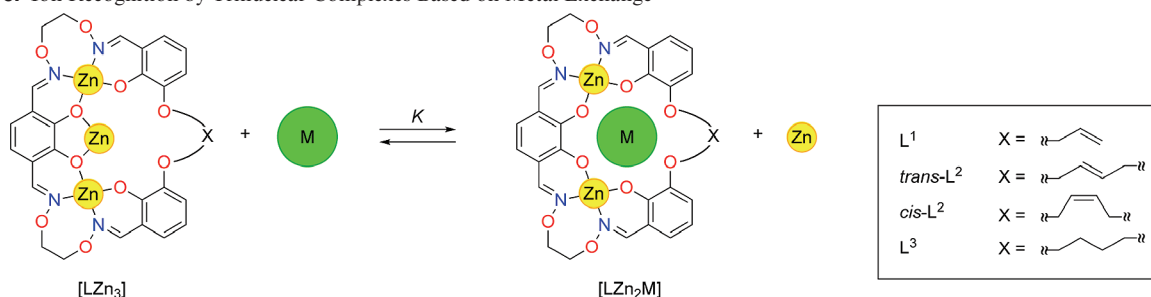


Table 4. Equilibrium Constants K for Metal Exchange of $[LZn_3]$ by Guest Ions^a

trinuclear complex	guest M			
	$La(NO_3)_3$	$Mg(OAc)_2$	$Ca(OAc)_2$	$Ba(OAc)_2$
$[L^1Zn_3]$	> 1000 [100%] ^b	1.2(2) [50%]	100 [91%] ^b	7(2) [70%]
$[(trans-L^2)Zn_3]$	> 1000 [100%] ^b	0.19(1) [27%]	0.20(2) [30%]	60 [89%] ^b
$[(cis-L^2)Zn_3]$	> 1000 [98%] ^b	0.011(2) [8%]	> 1000 [100%] ^b	> 1000 [100%] ^b
$[L^3Zn_3]$	> 1000 [100%] ^b	0.015(3) [9%]	400 [95%] ^b	600 [96%] ^b

^a The equilibrium constants were determined by non-linear least-squares analysis. Standard deviation is given in parentheses. The mole fraction of $[LZn_2M]$ upon the addition of guest M (1 equiv) is given in brackets. ^b The equilibrium constants were roughly estimated by the above-mentioned mole fractions.

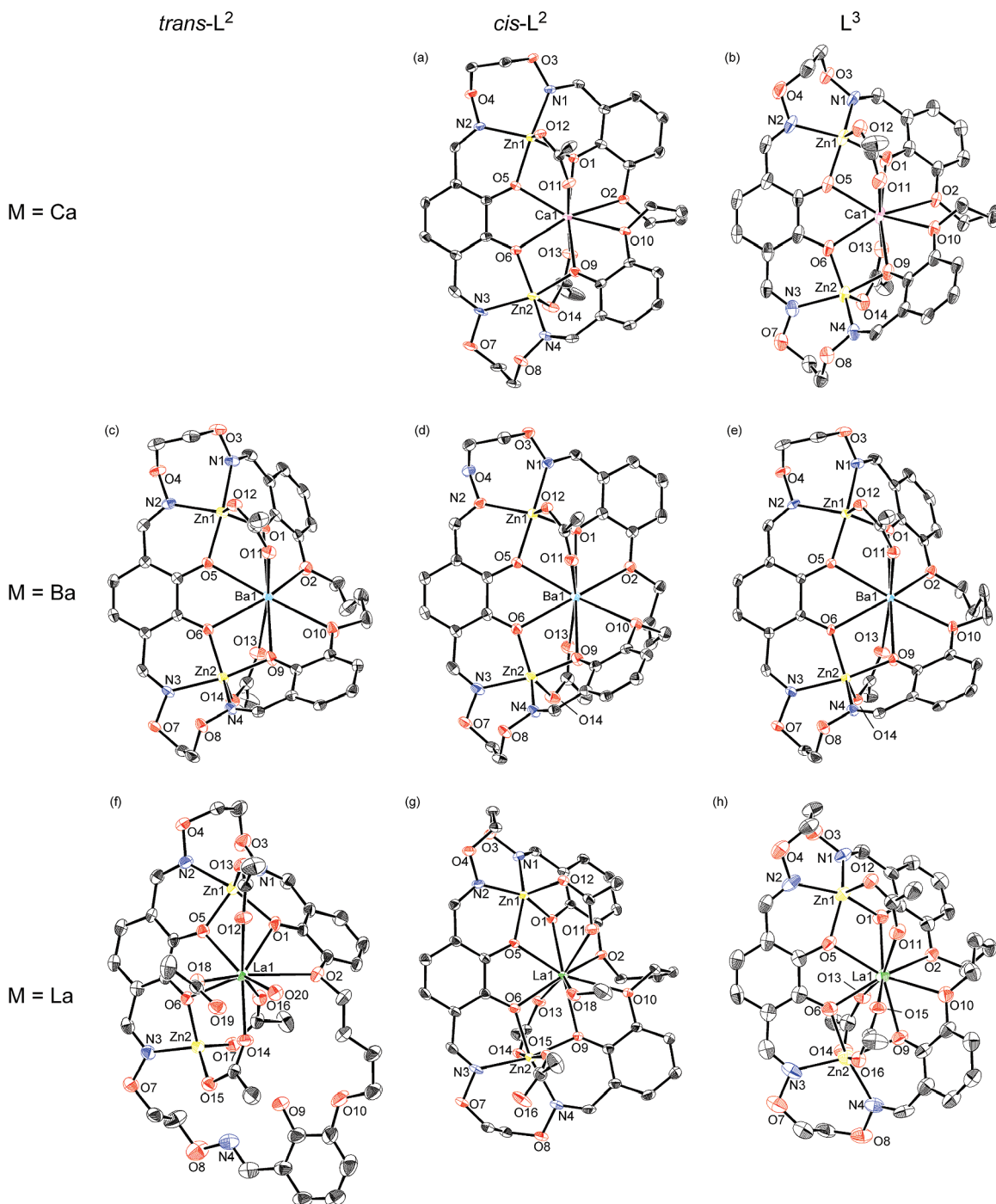


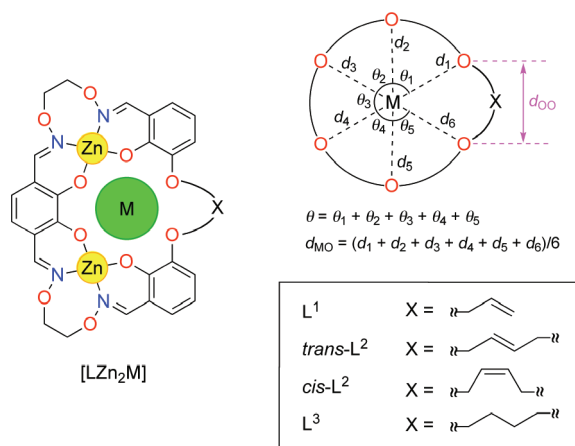
Figure 5. Crystal structure of trinuclear complexes (a) [(*cis*-L²)Zn₂Ca(OAc)₂], (b) [L³Zn₂Ca(OAc)₂], (c) [(*trans*-L²)Zn₂Ba(OAc)₂], (d) [(*cis*-L²)Zn₂Ba(OAc)₂], (e) [L³Zn₂Ba(OAc)₂], (f) [(*trans*-HL²)Zn₂La(OAc)₄], (g) [(*cis*-L²)Zn₂La(OAc)₃], and (h) [L³Zn₂La(OAc)₃] with thermal ellipsoids drawn at 50% probability level. Hydrogen atoms, disordered atoms, and solvent molecules are omitted for clarity.

(Figure 5c–e). The distances d_{OO} of these complexes are in the range of 3.7–4.4 Å, which are longer than those of [(*cis*-L²)Zn₂Ca(OAc)₂] and [L³Zn₂Ca(OAc)₂] (around 2.8 Å). In particular, the cavity size of the *trans*-L² is suitable for the inclusion of a barium ion. The distance d_{OO} of [(*trans*-L²)Zn₂Ba(OAc)₂] (4.3 Å) is nearly the same as that of the acyclic analogue [L¹Zn₂Ba(OAc)₂] (4.4 Å), which does not have a constraint because of a cyclic skeleton. This indicates that the [(*trans*-L²)Zn₂] moiety can accommodate a barium ion without any significant strain. The larger cavity of *trans*-L² accounts

for the high Ba²⁺/Ca²⁺ selectivity of the metal exchange of [(*trans*-L²)Zn₃]. In contrast, the distance d_{OO} of [(*cis*-L²)Zn₂Ba(OAc)₂] was shorter (3.7 Å). In the case of the saturated analogue [L³Zn₂Ba(OAc)₂], the distance (d_{OO} = 4.1 Å) is nearly the same as that of [(*trans*-L²)Zn₂Ba(OAc)₂] (d_{OO} = 4.3 Å). The conformation of the tetramethylene moiety is all-*anti*. This is well contrasted with the *gauche* conformation in [L³Zn₂Ca(OAc)₂] with a shorter d_{OO} (2.8 Å). As a result, the metal exchange of [L³Zn₃] by Ca²⁺ or Ba²⁺ highly efficiently takes place in an induced-fit fashion, because the [L³Zn₂]

Table 5. Geometrical Parameters of Metallohost-Guest Complexes [LZn₂M] (L = L¹, *cis*-L², *trans*-L², L³; M = Ca²⁺, Ba²⁺, La³⁺)

complex		distance (Å)		winding angle
		<i>d</i> _{OO} ^a	<i>d</i> _{MO} ^b	θ (deg) ^c
[L ¹ Zn ₂ Ca(OAc) ₂]	(A) ^d	3.150	2.496	314.8
	(B) ^d	3.093	2.469	319.7
[(<i>cis</i> -L ²)Zn ₂ Ca(OAc) ₂]		2.787	2.477	316.1
[L ³ Zn ₂ Ca(OAc) ₂]		2.860	2.473	319.0
[L ¹ Zn ₂ Ba(OAc) ₂]	(A) ^d	4.360	2.747	293.8
	(B) ^d	4.443	2.761	290.5
[(<i>trans</i> -L ²)Zn ₂ Ba(OAc) ₂]		4.267	2.812	286.9
[(<i>cis</i> -L ²)Zn ₂ Ba(OAc) ₂]		3.700	2.765	296.4
[L ³ Zn ₂ Ba(OAc) ₂]		4.136	2.783	291.1
[L ¹ Zn ₂ La(OAc) ₃]		3.361	2.583	315.8
[(<i>trans</i> -HL ²)Zn ₂ La(OAc) ₄]	(A) ^d	4.853, 5.083	3.679 ^e	— ^e
	(B) ^d	4.871	3.641 ^e	— ^e
[(<i>cis</i> -L ²)Zn ₂ La(OAc) ₃]		2.837	2.534	318.3
[L ³ Zn ₂ La(OAc) ₃]		3.173	2.559	320.3

^a Defined as the distance between the two ArOCH₂— oxygen atoms.^b Defined as the average of the six M—O distances *d*₁–*d*₆. ^c Defined as the sum of the five O—M—O angles θ₁–θ₅. ^d A and B denote crystallographically independent molecules. ^e Some oxygen atoms do not coordinate to M.

moiety changes its conformation and *d*_{OO} according to the size of the guest.

Zinc–lanthanum heterotrimeric complexes were also prepared from the three macrocyclic ligands H₄L (L = *trans*-L², *cis*-L², L³; Figure 5f–h). Among them, *cis*-H₄L² and H₄L³ formed trinuclear complexes [LZn₂La(OAc)₃] (L = *cis*-L², L³) with a structure analogous to the [LZn₂Ca(OAc)₂]. However, *trans*-H₄L² produced a different type of complex upon the reaction with zinc(II) acetate and lanthanum(III) acetate. The obtained complex was [(*trans*-HL²)Zn₂La(OAc)₄], in which one of the salicylaldoxime moieties does not participate in the

coordination. As a result, the La³⁺ does not fit into the central O₆ site. This is mainly attributed to the conformational constraint of the *trans*-olefin moiety, which prohibits coordination of all the oxygen atoms.

Conclusion

The new acyclic tetraoxime ligand, H₄L¹, having two terminal allyl groups was designed and synthesized. The terminal allyl groups were introduced so that the olefin metathesis can convert H₄L¹ into the cyclic derivatives, *trans*-H₄L², *cis*-H₄L², and then the saturated analogue, H₄L³, by hydrogenation. The cyclic *trans*-H₄L² ligand was selectively obtained via the olefin metathesis of H₄L¹, while the reaction of [L¹Zn₂Ca] exclusively afforded *cis*-H₄L². The complexation of the H₄L ligands (L = L¹, *trans*-L², *cis*-L², L³) with zinc(II) acetate (3 equiv) yielded the trinuclear complexes [LZn₃]. The trinuclear complex of the acyclic ligand ([L¹Zn₃]) was formed in a highly cooperative fashion. On the other hand, macrocyclic ligands (L = *trans*-L², *cis*-L², L³) first gave the intermediate 2:3 complex [(HL)₂Zn₃] and then the trinuclear complexes [LZn₃]. Spectroscopic investigation showed that the trinuclear complexes [LZn₃] (L = L¹, *trans*-L², *cis*-L², L³) can recognize alkaline earth metal ions via the site-selective metal exchange. The acyclic [L¹Zn₃] and cyclic [(*trans*-L²)Zn₃] showed the opposite Ca²⁺/Ba²⁺ selectivity. The metal exchange of [LZn₃] with La³⁺ quantitatively took place to give [LZn₂La], but the number of coordinating oxygen atoms in the crystal of [(*trans*-HL²)Zn₂La(OAc)₄] was different from those in other complexes. Consequently, the complexation behavior of the tetraoxime ligands significantly changes by linking of the terminal olefinic moieties of H₄L¹ and the linking structure (*trans*-, *cis*-olefin, and saturated). The transformation using olefin metathesis is useful to modulate the complexation behavior of multidentate ligands, because the olefin metathesis and hydrogenation take place under mild conditions. The transformation would also be useful for fine-tuning of the chemical or physical properties of the oligometallic core, such as the catalytic activity or redox and magnetic properties.

Acknowledgment. We thank Dr. Kenji Yoza (Bruker AXS KK) for the X-ray data collection of *trans*-H₄L² and *cis*-H₄L². This work was supported by Grants-in-Aid for Scientific Research from the Ministry of Education, Culture, Sports, Science and Technology, Japan.

Supporting Information Available: X-ray crystallographic data in CIF format. This material is available free of charge via the Internet at <http://pubs.acs.org>.